- Technical Paper -

EXPERIMENT ON BUCKLING BEHAVIOR OF ULTRA-HIGH STRENGTH REBARS IN RC COLUMN

Aixin ZHOU[*1], Yuping SUN[*2], Takashi TAKEUCHI[*3] and Pengjun LUO[*4]

ABSTRACT

Twelve square columns reinforced by SD345 or SBPDN rebars were tested under axially compressive load to investigate the buckling behavior of ordinary and ultra-high strength rebars in reinforced concrete (RC) columns. Test results indicated that the slenderness ratio of 8 is sufficient to prevent premature buckling of SD345 rebars. Whereas, the SBPDN rebars may buckle before yielding even the slenderness ratio was as small as 4. This fact implies that stronger lateral restraint is required to achieve satisfactory post yielding behavior of ultra-high strength rebars.

Keywords: Ultra-high strength rebar, Compression, Buckling, Slenderness ratio, RC column

1. INTRODUCTION

The buckling of longitudinal rebars is commonly reported in reinforced concrete (RC) columns that exposed to severely seismic load. In the RC columns that with inadequately spaced stirrups, due to the insufficient lateral restrains, the premature buckling of the longitudinal rebars usually occurs under a critical level of compressive strain after the concrete cover spalls. Owing to the weaker capacity of the buckled longitudinal rebars in resisting the axial deformations, the occurrence of the bar buckling usually signs the initiation of degradation in axial deformation performance of columns. Consequently, the study concerning on the issue of longitudinal rebar buckling has drawn much attention.

For instance, Monti and Nuti experimentally and theoretically studied the stress-strain relations of the compressed bare rebars with considering the inelastic buckling effects [1]. It was found that the ratios of unsupported length to rebar diameter significantly affect the post-buckling behavior of compressed rebars. Especially, the critical ratio, which is the maximum ratio for sufficiently achieving the satisfactory post-yielding behavior, was reported to be six. Bae et al. also obtained the similar conclusions based on the test results of 162 bare rebar specimens [2]. The inelastic buckling of smooth bare rebars and the ultra-high strength bare rebars were also investigated by some other researchers [3, 4].

These previous researches, however, mainly investigate the buckling behavior of bare rebars under the approximately ideal fixed supports with enough stiffness. In the RC columns, the longitudinal rebars are usually only restrained by closely spaced lateral stirrups. The lateral stiffness provided by the stirrups is likely to be much less than the fixed supports. Under compressive loads, moreover, RC columns tend not only to shorten lengthwise but also to expand laterally due to the Poisson effect. These effects may result in the buckling behavior of the longitudinal rebars that embedded in RC columns differs from that of the isolated rebars [5,6]. In addition, the ultra-high strength rebars have been more and more widely introduced to the construction of civil structures due to their superior physical and mechanical properties. The utilization of SBPDN rebars to achieve the highly resilient concrete components is one of the typical examples [7]. To date, however, the comparison study between the buckling behavior of ordinary and ultra-high strength rebars embedded in RC columns is, if any, few.

The primary objective of the present study is to experimentally investigate the buckling behavior of SD345 and SBPDN rebars in square RC columns under axially compressive load. The effect of lateral stirrup spacing on the buckling of longitudinal rebars is also considered. The observations obtained from the tests are expected to provide some insights into the design of RC components reinforced by ultra-high strength rebars.

2. EXPERIMENTAL PROGRAM

2.1 Test Specimens

A total of 12 square columns, each had an identical cross-section of 150 mm and a height of 300 mm, were manufactured in the present study. Among 12 specimens, half were reinforced with ordinary strength reinforcement rebars (i.e., SD345) and the other half were reinforced with ultra-high strength reinforcement rebars (i.e., SBPDN). The nominal diameters of SD345

*1 Graduate Student, Graduate School of Engineering, Kobe University, JCI Student Member
*2 Professor, Graduate School of Engineering, Kobe University, JCI Member
*3 Assistant Professor, Graduate School of Engineering, Kobe University, JCI Member
*4 Graduate Student, School of Civil Engineering, Southwest Jiaotong University, JCI Student Member

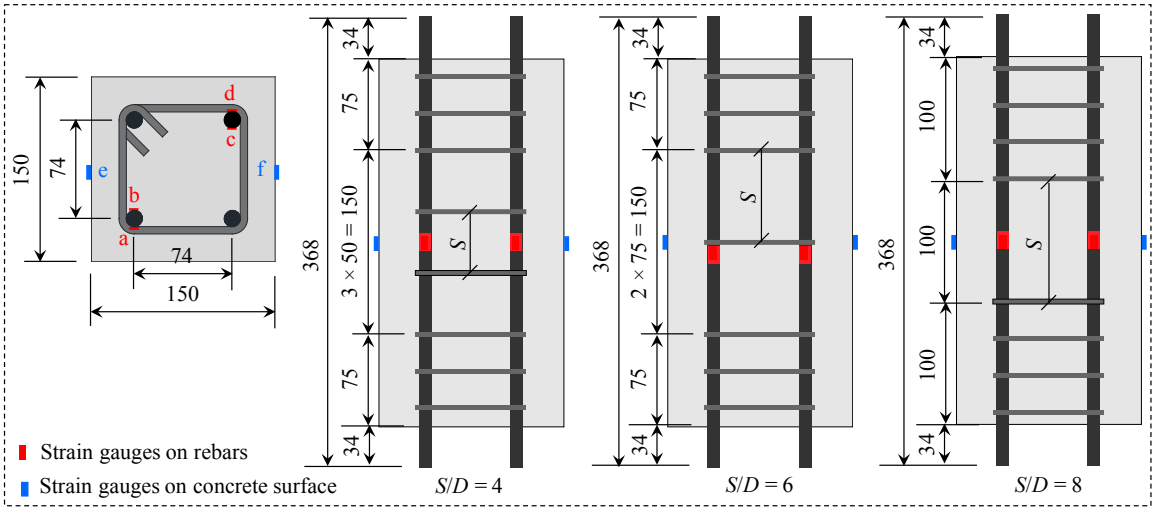

(a) Type-A arrangement

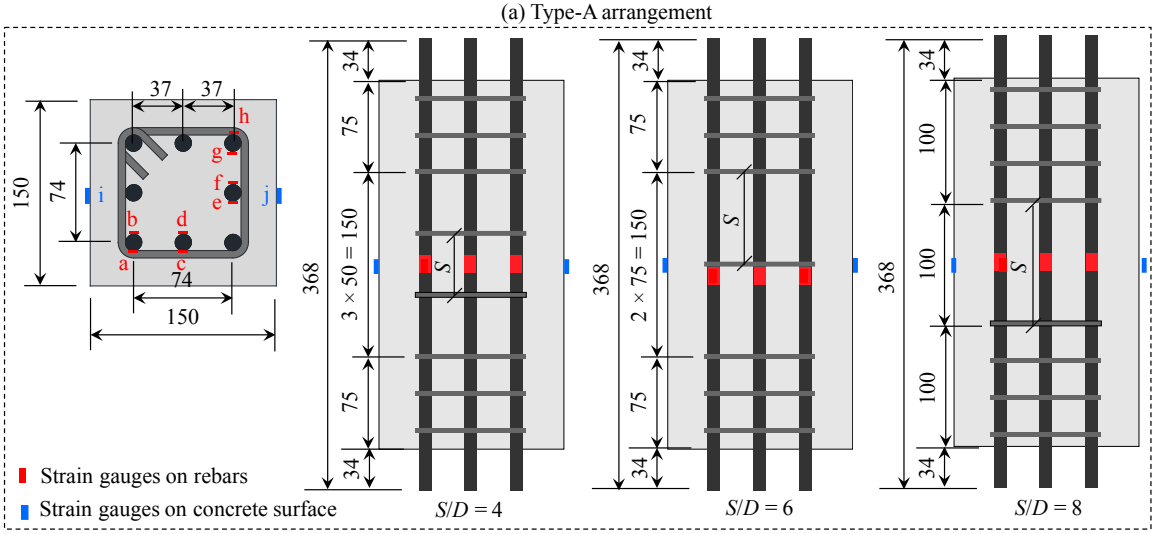

(a) Type-B arrangement

Fig.1 Configurations of test specimens (unit: mm)

rebar and SBPDN rebar are 13.0 mm and 12.6 mm, respectively. As shown in Fig. 1, two arrangements of longitudinal rebar (named as Type-A and Type-B, respectively, hereafter) were used in the test. Type-A arrangement [Fig. 1(a)] that consists of 4 rebars (with each rebar be arranged at a corner of the square section) was used for all six specimens reinforced by SPBDN as well as three specimens reinforced by SD345. The center-to-center distance of two adjacent longitudinal rebars was specified as 74 mm in Type-A arrangement. In addition to the same reinforcement configuration as that of Type-A, four additional rebars were added in Type-B arrangement [Fig. 1(b)]. Each additional rebar was placed at the midpoint between the two-adjacent corner rebars, which resulted in the center-to-center distance of two adjacent longitudinal rebars to be 37 mm. Type-B arrangement was used to three specimens reinforced by SD345. The lateral stirrups, which were made from SD295 deformed steel round rebars with a nominal diameter of 6.5 mm, were used to confine the concrete core and longitudinal rebars. Defining the slenderness ratio (S/D) of longitudinal rebar as the ratio of stirrup spacing (S) to the longitudinal rebar diameter (D). Since the critical value of S/D was widely observed to be six to achieve a post-yield buckling behavior of longitudinal rebar by several researchers [1,2]. In order to investigate the effect of the slenderness ratios, therefore, S was designed to be 50 mm, 75 mm, and 100 mm to yield S/D values approximately to be 4, 6, and 8, respectively. At two ends of each specimen, stirrup spacing decreased to 30 mm to ensure that the buckling of rebars would occur at the middle region of the columns. The rebars also extended outside with 34 mm at the ends of each specimen for the ease of specimen fabrication and load application. Fig. 1 also shows the layout of the strain gauges attached on the longitudinal bars and the surface of concrete cover. Two strain gauges were attached on the opposite sides of the longitudinal bar at mid-height section to attempt to monitor the onset of the bar buckling. In the following text, the specimens are named using the form such as “4S50” or “H4S50”, in which, “4” represents the number of the longitudinal rebars, “S50” represents the stirrup spacing of 50 mm, and the “H” means that ultra-high strength rebars were used. Notably, two identical specimens reinforced by SBPDN are respectively indicated by “A” or “B”, for instance, “H4S50A” and “H4S50B”.

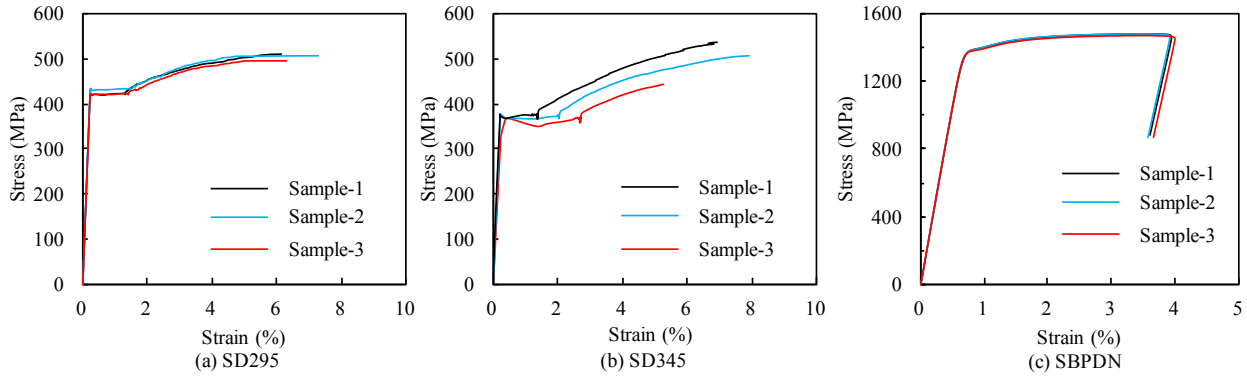

Fig.2 Tensile stress-strain curves of rebars

2.2 Material Properties

The tested tensile stress-strain relationships of SD295, SD345, and SBPDN steel rebars are shown in Fig. 2(a), 2(b), and 2(c), respectively. The average values of mechanical properties from three samples are listed in Table. 1.

Ready-mixed concrete made of Portland cement and coarse aggregates with maximum particle size of 20 mm was used to fabricate the specimens. The average concrete compressive and splitting tensile strengths respectively obtained from three cylinders (100 mm in diameter and 200 mm in height) at 28 days were 41.0 MPa and 3.4 MPa. The corresponding Young's modulus and peak strain are 26.1 GPa and 0.0026, respectively. The mean value of the actual concrete compressive strength at the time of testing was 43.3 MPa with a standard deviation of 1.9 MPa.

2.3 Loading Method and Measurement

Fig. 3 shows the photograph of the test setup. All the specimens were subjected to monotonic compression load using a universal testing machine with a capacity of 2000 kN. Steel plates were placed at both ends of the specimen in order to provide loads for concrete and rebars simultaneously. The rebars were anchored by nuts to the end 34mm-thick steel plates. A load cell was used to measure the magnitude of the load applied. Four linearly variable differential transformers (LVDTs), which were located at the corners of the specimen, were used to measure the overall axial displacements. The tests were stopped when the axial shortening reached to 3% of the length of the specimen (i.e., average overall axial displacement of 9 mm).

Table 1 Mechanical properties of rebars

Grade	D (mm)	E_s (GPa)	f_y (MPa)	f_u (MPa)	ε_y (%)	ε_{sh} (%)
SD295	6.5	189	421	528	0.22	1.36
SD345	13.0	180	374	539	0.21	1.84
SBPDN	12.6	211	1413*	1477	0.86*	/

Note: D = Diameter; E_s = Young's modulus; f_y = Yield stress; f_u = Tensile stress; ε_y = Yield strain; ε_{sh} = Strain at starting point of hardening branch; * based on the 0.2% offset method.

3. TEST RESULTS AND DISCUSSIONS

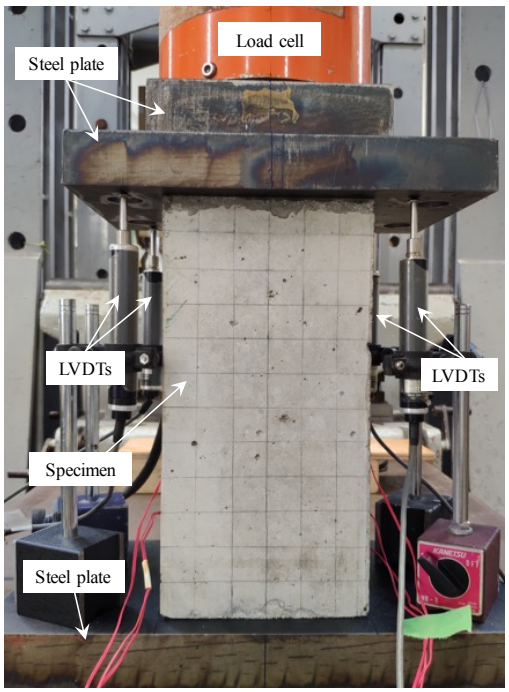

Fig.3 Photograph of test setup

3.1 Observed Damage Processes

Observations during the test suggest that the damage processes were similar in all twelve specimens tested. It was observed that the typical damage processes of each specimen can be roughly divided into four stages, as indicated in Fig. 4. Stage I is defined as the initial stage, at which no visible cracks were detected on the surface (or only micro cracks occurred) and the axial load could reach about 600 kN to 800 kN for the specimens reinforced by SD345 rebars and could reach about 1000 kN for the specimens reinforced by SBPDN rebars. The specimens exhibited approximately linear elastic behavior at this stage. At stage II, then, noticeably vertical surface cracks occurred in the cover concrete at the regions in the vicinity of the longitudinal bars. The stiffness of the columns began to decrease owing to the presence of these principal vertical cracks. In addition, according to the measurement by strain gauges that attached on the rebars (i.e., red marks in Fig. 1), SD345 rebars were observed yielding but SBPDN rebars still remained elastic in this stage. Next, the principal cracks started to

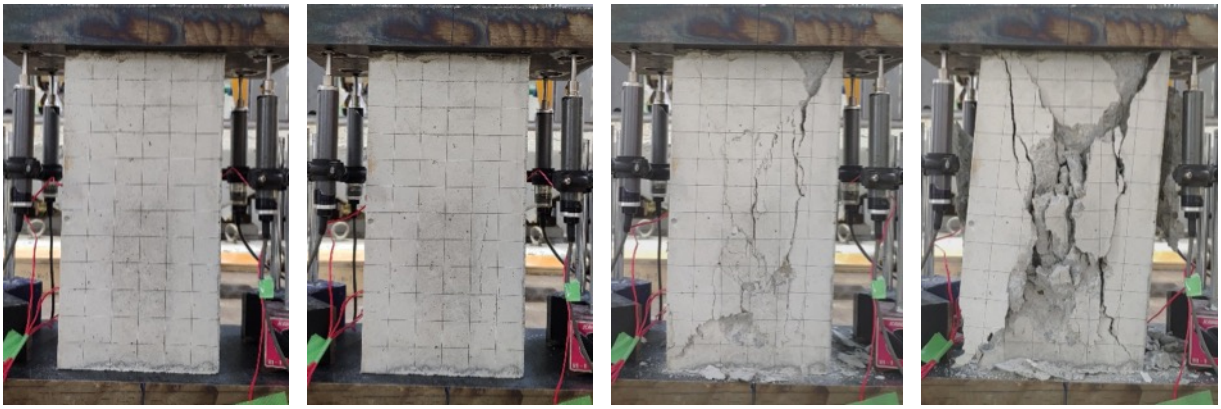

(a) Stage I (b) Stage II (c) Stage III (d) Stage IV

Fig.4 Typical damage processes (taking specimen 4S100 as the instance)

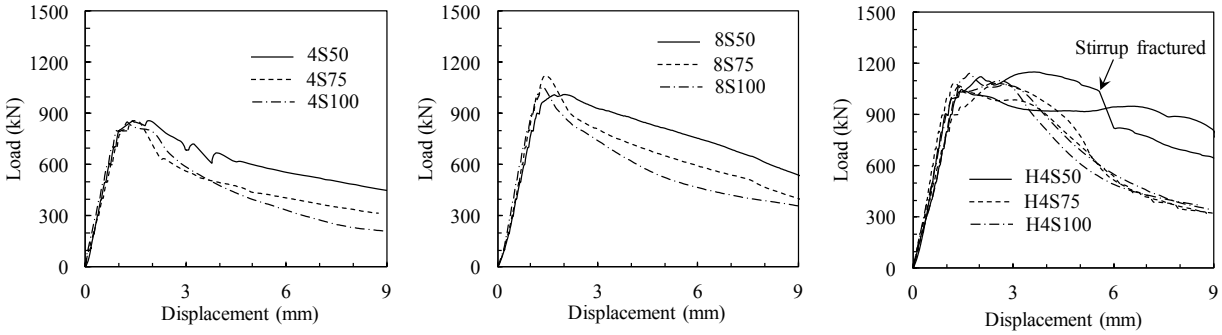

Fig.5 Load-displacement curves

spread and widened as the axial load increased and the columns reached its capacity at stage III. Meanwhile, some of the monitored longitudinal bars buckled, which resulted in the cover concrete bulging out from the main column and subsequently spalling. The measurements by the strain gauges that attached on concrete surface (blue marks in Fig. 1) also indicated that the concrete cover unloaded at this stage. The corresponding average axial strain of the concrete was about 0.0015 to 0.0030. Finally, the tests were continued until the average axial displacement reached to 9 mm, which corresponds to the longitudinal strain of 0.03. The cover concrete at mid-height region of the column destroyed completely. The load was carried by the core concrete and the longitudinal bars that had extensively buckled. Noting that the lateral stirrup in some specimens fractured accompanying with the loud voice at stage IV, which may be primary induced by the expansion of core concrete and outwards deformation of the buckled longitudinal bars.

3.2 Load-Displacement Curves

Fig. 5 shows the load-displacement curves of all the tested columns. In these figures, the load is obtained from the load cell and the displacement is the average value obtained from the four LVDTs (see Fig. 3). As can be seen, all the curves are linear at the initial stage, and then the stiffness gradually deceases due to the yielding of the longitudinal bar and the appearance of the vertical concrete cracks. The stirrup spacing was observed to have only slight effect on the load capacity of the specimen, but it significantly affects the descending branch after the peak points. For instance, the peak loads of the specimens 4S50, 4S75, and 4S100, are 857 kN, 862 kN, and 851 kN, respectively, which only have very slight difference. After these peak points, however, the slope decreases faster in the specimen with larger stirrup spacing. This leads to the residual load-carrying capacities (i.e., the load-carrying capacity at the end of test) of each specimen as 450 kN (4S50), 311 kN (4S75), and 208 kN (4S100), respectively. This also implies that the small stirrup spacing improved the deformation performance of the columns. In addition, comparing the curves of the specimens reinforced by SD345 rebars with that of the specimens reinforced by SBPDN rebars, the sharper drop in axial resistance of the SD345 reinforced specimens was observed after the peak points. This is mainly because of that the ultra-high strength steel rebars remained elastic when the column reached its load capacity, the strength reduction induced by the core concrete damage would be supported by the SBPDN rebars. Furthermore, for the specimen H4S50A, one stirrup fractured when during the test, which resulted in a sharp drop in the load-displacement curve. The peak loads (P_{max}) and the corresponding average overall axial displacements (Δ) of all the specimens are listed in Table 2.

3.3 Longitudinal Bar Buckling

Fig. 6 shows the tested columns after removing the damaged surrounding concrete. As expected, all the longitudinal bars buckled at the mid-region of the columns. For the specimens with stirrup spacing of 50 mm (S/D = 4), the longitudinal bars buckled in the length of two (4S50 and H4S50A) or three (8S50 and H4S50B) intervals. For the specimens with stirrup

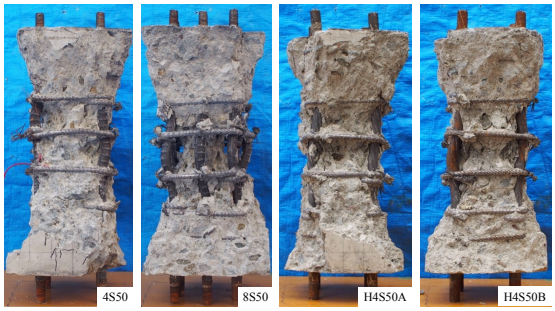

(a) specimens with S/D = 4

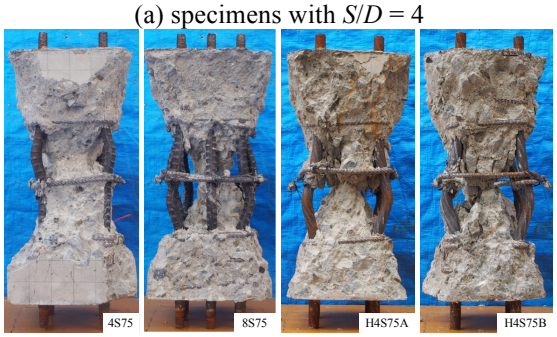

(b) specimens with S/D = 6

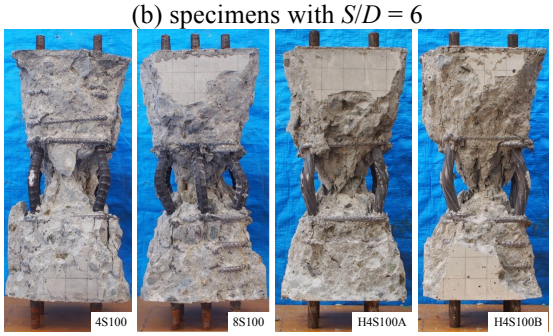

(c) specimens with S/D = 8

Fig.6 Buckled longitudinal rebars

spacing of 75 mm (S/D = 6), the longitudinal bars buckled in the length of one (4S75) or two (8S75, H4S75A, and H4S75B) intervals. For the specimens with stirrup spacing of 100 mm (S/D = 8), all the longitudinal bars buckled in the length of one interval. It was also observed the core concrete damaged more serious in the specimens with larger stirrup spacing. Since all the specimens were loaded up to the same ultimate overall axial displacement of 9 mm, the above-mentioned observation with respect to the core concrete damage can reasonably explain the higher residual load-carrying capacities of the specimens with denser stirrup arrangement.

Fig. 7 and 8 respectively illustrate the typical relationships of the measured strains and the average axial displacement for SD345 and SBPDN rebars in the columns. The negative values of the ordinate represent the compression. For ordinary strength rebars (see Fig. 7), the measured strains increased linearly at the elastic stage; afterward, the strains reached to the yield plateau. During these stages, the measured strains by the strain gauge pairs attached on the opposite sides were almost identical. However, the strains began to deviate from each other before they reached the starting point of hardening branch (ε_{sh}), indicating that the longitudinal rebars began to bend. Thus, the second turning points

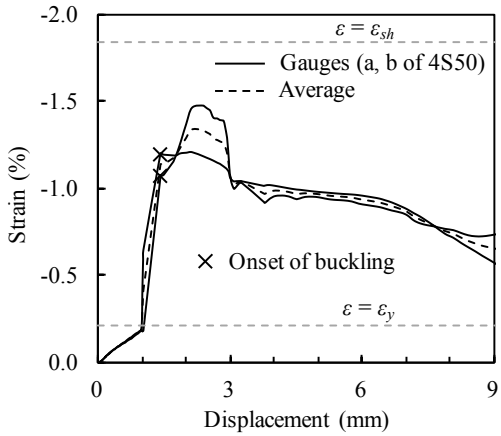

Fig.7 Strain-displacement curves of SD345 rebar

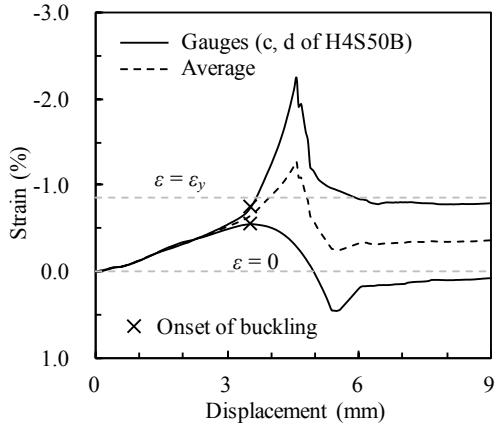

Fig.8 Strain-displacement curves of SBPDN rebar

were defined as the onset of buckling. For ultra-high strength rebars (see Fig. 8), the measured strains by the strain gauge pairs attached on the opposite sides were also almost identical and increased linearly at the early stage. Afterward, the strains began to deviate from each other, which also indicated the bending of the longitudinal rebars. Thus, the reversal points of the strain were defined as the onset of buckling.

Table 2 lists the average strains (ε_b) of each rebars at the onset of buckling for all the tested columns. The corresponding axial loads (P_b), average axial displacement (Δ_b), and the number of buckled intervals (n) are also summarized in Table 2. The buckling strains of the rebars in the columns that reinforced by SD345 range from 0.21% to 1.52%, which locate on the yield plateau of the tensile stress-strain curves of SD345. This implies that the slenderness ratio (S/D) of 8 is sufficient to prevent premature bar buckling. In contrast, the buckling strains of SBPDN range from 0.33% to 0.89%, and most of them are smaller than their ε_y (i.e., 0.86%) that obtained from the tensile stress-strain curves, indicating that the SBPDN rebars buckled prematurely in the linearly elastic stage. The lower buckling strains of the ultra-high strength rebars can be attributed to the fact that the SBPDN rebars buckled at the linearly elastic stage while the SD345 rebars buckled at the yield plateau stage. Since the stirrups of theses specimens were made from SD295 deformed steel round rebars with a nominal diameter of

6.5 mm, which are usually used to restrain the ordinary strength longitudinal rebars. The lateral restraint provided by these traditional stirrups were insufficient to achieve post yielding behavior for SBPDN rebars, even though the stirrup spacing was specified as small as 50 mm.

Table 2 Summary of primary test results

Specimen	P_{max} (kN)	Δ (mm)	ε_b (%)	P_b (kN)	Δ_b (mm)	n
4S50 (44.5*)	857	1.43	1.14	857	1.43	2
			1.12	829	2.14	2
4S75 (44.5*)	862	1.47	0.90	803	1.25	1
			0.41	781	1.84	1
4S100 (44.5*)	851	1.26	0.21	799	0.94	1
			1.18	795	2.00	1
8S50 (43.8*)	1016	2.00	0.74	968	1.32	2
			1.16	989	1.47	2
			0.58	995	1.52	3
			0.92	997	1.53	2
8S75 (43.8*)	1126	1.40	1.31	1119	1.50	2
			0.90	1093	1.62	2
			0.63	1052	1.73	2
			0.94	900	2.18	2
8S100 (43.8*)	1057	1.34	0.59	1002	1.22	1
			1.52	934	1.73	1
			1.12	919	1.79	1
			1.25	919	1.79	1
H4S50A (43.2*)	1046	1.44	0.30	1007	2.27	2
			0.38	963	2.85	2
H4S50B (43.2*)	1154	3.52	0.53	1138	3.07	2
			0.67	1154	3.59	3
H4S75A (43.2*)	1085	1.16	0.57	987	2.89	2
			0.66	894	4.02	2
H4S75B (43.2*)	1085	2.57	0.72	1042	3.53	2
			0.86	974	4.18	2
H4S100A (44.6*)	1142	1.69	0.55	1065	3.18	1
			0.89	1053	3.32	1
H4S100B (44.6*)	1097	2.54	0.79	1088	2.84	1
			0.59	1086	3.27	1

Note: *The actual concrete compressive strength at the time of testing (in a unit of MPa).

4. CONCLUSIONS

Based on the test of twelve square columns, the following conclusions can be drawn:

(1) The similar damage processes were observed both in the columns reinforced by SD345 and SBPDN longitudinal rebars.

(2) The stirrup spacing has no obvious effect on the load-carrying capacity but greatly affects post-peak behavior of the axially compressed column. The smaller stirrup spacing is benefit to improve the deformation performance and residual load-carrying capacity.

(3) For the columns reinforced by SD345 rebars (f_y = 376 MPa), the slenderness ratio (S/D) of 8 is sufficient to prevent premature bar buckling, which makes it possible to achieve satisfactory post-yielding behavior under compression. Whereas, for the columns reinforced by SBPDN (f_y = 1413 MPa), even the slenderness ratio was specified to be as small as 4, the bar buckling was also observed before yielding.

(4) The more reasonable stirrup arrangement is necessary to be developed to achieve satisfactory post yielding behavior of ultra-high strength rebars, which is the focus of the further research.

ACKNOWLEDGEMENT

This work was supported by JSPS Grant No. R2904 in the Program for Fostering Globally Talented Researchers. The SBPDN rebars provided by Neturen Co. Ltd is also greatly appreciated.

REFERENCES

[1] Monti, G., Nuti, C. “Nonlinear cyclic behavior of reinforcing bars including buckling.” Journal of Structural Engineering, Vol. 118(12), 1992, pp. 3268-3284.

[2] Bae, S., Mieses, A.M., Bayrak, O. “Inelastic buckling of reinforcing bars.” Journal of Structural Engineering, Vol. 131(2), 2005, pp. 314-321.

[3] Cosenza, E., Prota, A. “Experimental behaviour and numerical modelling of smooth steel bars under compression.” Journal of Earthquake Engineering, Vol. 10(03), 2006, pp. 313-329.

[4] Hu, M.H., Han, Q., Xu, K., Du, X.L. “Corrosion influences on monotonic properties of ultra-high-strength reinforcing steels.” Construction and Building Materials, Vol. 198, 2019, pp. 82-97.

[5] Pantazopoulou, S.J. “Detailing for reinforcement stability in RC members.” Journal of Structural Engineering, Vol. 124(6), 1998, pp. 623-632.

[6] Dhakal, R.P., Su, J. “Design of transverse reinforcement to avoid premature buckling of main bars.” Earthquake Engineering & Structural Dynamics, Vol. 47(1), 2018, pp. 147-168.

[7] Sun, Y.P., Cai, G.C., Takeshi, T. Seismic behavior and performance-based design of resilient concrete columns.” International Journal of Applied Mechanics and Materials, Vol. 438, 2013, pp. 1453-1460.

[8] Liao, C.L., Mau, S.T. “Inelastic post buckling behavior of very short column.” Journal of the Chinese Institute of Engineers, Vol. 8(4), 1985, pp. 333-341.